

Searching for nontensorial polarizations of stochastic gravitational waves with laser interferometers

Atsushi Nishizawa^{1(a)}, Atsushi Taruya^{(b),(c)}, Kazuhiro Hayama^{(d),(e)}, Seiji Kawamura^(d),
Masa-aki Sakagami^(f)

^(a)*Division of Theoretical Astronomy, National Astronomical Observatory of Japan, Mitaka, Tokyo 181-8588*

^(b)*Research Center for the Early Universe, School of Science, The University of Tokyo, Tokyo 113-0033*

^(c)*Institute for the Physics and Mathematics of the Universe, University of Tokyo, Kashiwa, Chiba 277-8568*

^(d)*TAMA Project, National Astronomical Observatory of Japan, Mitaka, Tokyo 181-8588*

^(e)*Albert-Einstein-Institut (Max-Planck-Institut für Gravitationsphysik), Callinstraße 38, D-30167 Hannover, Germany*

^(f)*Graduate School of Human and Environmental Studies, Kyoto University, Kyoto 606-8501*

Abstract

In general relativity, a gravitational wave (GW) has two polarization modes, while in modified gravity, the GW is allowed to have additional polarizations. Thus, the observation of the GW polarizations can be utilized for the test of gravity theories. In this article, we investigated the mode-separability and detectability of additional polarization modes of gravitational waves, particularly focusing on a stochastic gravitational-wave background, with laser-interferometric detectors based on the ground and space. As a result, we found that the additional polarization modes can be successfully separated and detected.

1 Introduction

General relativity (GR) has been strictly tested in the solar system [1, 2], however, has not been strongly constrained at a cosmological scale and in a strong field regime. If the gravity theory is deviated from GR, it gives rise to various observational signatures. The properties of a gravitational wave (GW) are also altered in the propagation speed, waveforms, and polarization modes. In GR, a GW has two polarization modes (plus and cross modes), while in a general metric theory of gravitation, the GW is allowed to have, at most, six polarizations [1, 3]. Such additional polarizations appear in modified gravity and extra-dimensional theories, corresponding to extra degrees of freedom in the theories. Therefore, the observation of the GW polarizations can be utilized for the test of the gravity theory.

Currently, there are a few observational constraints on the additional polarization modes of GWs. For the scalar GWs, the observed orbital-period derivative of PSR B1913+16 agrees well with the predicted values of GR, conservatively, at a level of 1% error [2], indicating that the contribution of scalar GWs to the energy loss is less than 1%. On the other hand, a null result in a search for a stochastic gravitational-wave background (GWB) by LIGO [4] has given an upper limit on an energy density, $h_0^2 \Omega_{\text{gw}} \lesssim 3.6 \times 10^{-6}$. No detection can also be applied to non-Einsteinian polarizations, though a factor of the upper limit would be corrected, depending on a detector response.

In this article, we focus on the stochastic GWB here and investigate the separability of the polarization modes of the GWB with laser-interferometric detectors.

2 GW polarizations and cross-correlation analysis

Using the unit vectors $\hat{\mathbf{m}}$ and $\hat{\mathbf{n}}$ perpendicular to the unit vector pointing at the GW propagation direction $\hat{\mathbf{\Omega}}$ and to each other, the polarization tensors for $p = +, \times, b, \ell, x$, and y called plus, cross, breathing,

¹Email address: atsushi.nishizawa@nao.ac.jp

longitudinal, vector-x, and vector-y modes, respectively, are defined by [1, 3]: $\mathbf{e}_+ = \hat{\mathbf{m}} \otimes \hat{\mathbf{m}} - \hat{\mathbf{n}} \otimes \hat{\mathbf{n}}$, $\mathbf{e}_\times = \hat{\mathbf{m}} \otimes \hat{\mathbf{n}} + \hat{\mathbf{n}} \otimes \hat{\mathbf{m}}$, $\mathbf{e}_b = \hat{\mathbf{m}} \otimes \hat{\mathbf{m}} + \hat{\mathbf{n}} \otimes \hat{\mathbf{n}}$, $\mathbf{e}_\ell = \sqrt{2} \hat{\Omega} \otimes \hat{\Omega}$, $\mathbf{e}_x = \hat{\mathbf{m}} \otimes \hat{\Omega} + \hat{\Omega} \otimes \hat{\mathbf{m}}$, $\mathbf{e}_y = \hat{\mathbf{n}} \otimes \hat{\Omega} + \hat{\Omega} \otimes \hat{\mathbf{n}}$. Each polarization mode is orthogonal to one another and is normalized so that $e_{ij}^p e_{p'ij}^{j'} = 2\delta_{pp'}$, $p, p' = +, \times, b, \ell, x, y$. The angular response function of the I-th interferometer is given by contraction of the polarization tensors with the detector tensors: $F_I^p(\hat{\Omega}) \equiv \mathbf{D}_I : \mathbf{e}_p(\hat{\Omega})$ and $\mathbf{D}_I \equiv [\hat{\mathbf{u}} \otimes \hat{\mathbf{u}} - \hat{\mathbf{v}} \otimes \hat{\mathbf{v}}]/2$. The unit vectors $\hat{\mathbf{u}}$ and $\hat{\mathbf{v}}$ are directed to each detector arm. Note that the above expression is valid only when the arm length of the detector, L , is much smaller than the wavelength of GWs, λ_g , in the observational frequency band we consider. This condition holds for both ground-based detectors and space-based detector such as DECIGO.

We assume that a stochastic GWB is (i) isotropic, (ii) independently polarized (not correlated between polarizations), (iii) stationary, and (iv) Gaussian. Conventionally, the amplitude of GWB for each polarization is characterized by $\Omega_{\text{gw}}^p(f) \equiv (d\rho_{\text{gw}}^p/d\ln f)/\rho_c$, where $\rho_c = 3H_0^2/8\pi G$ and $H_0 = 100 h_0 \text{ km sec}^{-1} \text{ Mpc}^{-1}$ [5–8]. Then, we define the GWB energy density in tensor, vector, and scalar polarization modes as $\Omega_{\text{gw}}^T \equiv \Omega_{\text{gw}}^+ + \Omega_{\text{gw}}^\times$, $\Omega_{\text{gw}}^V \equiv \Omega_{\text{gw}}^x + \Omega_{\text{gw}}^y$, $\Omega_{\text{gw}}^S \equiv \Omega_{\text{gw}}^b + \Omega_{\text{gw}}^\ell = \Omega_{\text{gw}}^b(1 + \kappa)$. Here we assume $\Omega_{\text{gw}}^+ = \Omega_{\text{gw}}^\times$ and $\Omega_{\text{gw}}^x = \Omega_{\text{gw}}^y$. For the scalar mode, we introduced a model-dependent parameter, $\kappa(f) \equiv \Omega_{\text{gw}}^\ell(f)/\Omega_{\text{gw}}^b(f)$.

To distinguish a stochastic GWB from detector random noise, one needs to correlate detector's signals [5–8]. We assume that the amplitude of GWB is much smaller than detector noise. In the cross-correlation analysis between I-th and J-th detectors, a GW signal can be written as

$$\mu = \frac{3H_0^2}{20\pi^2} T_{\text{obs}} \sin^2 \chi \int_{-\infty}^{\infty} df |f|^{-3} \tilde{Q}(f) \left[\Omega_{\text{gw}}^T(f) \gamma_{IJ}^T(f) + \Omega_{\text{gw}}^V(f) \gamma_{IJ}^V(f) + \xi(f) \Omega_{\text{gw}}^S(f) \gamma_{IJ}^S(f) \right],$$

where T_{obs} is observation time, $\tilde{Q}(f)$ is a filter function, which weight the correlation signal so that signal-to-noise ratio (SNR) is maximized. The parameter defined by $\xi(f) \equiv [1 + 2\kappa(f)]/3[1 + \kappa(f)]$ takes the value in the range $1/3 \leq \xi \leq 2/3$, depending on the ratio of the energy density in the longitudinal mode to the breathing mode. The prefactor, $\sin^2 \chi = 1 - (\hat{\mathbf{u}} \cdot \hat{\mathbf{v}})^2$, comes from the detector tensor with non-orthogonal detector arms. The sensitivity to the GWB with each polarization can be characterized by so-called overlap reduction functions (ORF) [9]

$$\gamma_{IJ}^M(f) \equiv \frac{1}{\sin^2 \chi} \int_{S^2} \frac{d\hat{\Omega}}{4\pi} e^{2\pi i f \hat{\Omega} \cdot \Delta \vec{X}/c} \mathcal{R}_{IJ}^M,$$

with $\mathcal{R}_{IJ}^T(\hat{\Omega}) \equiv (5/2) \times (F_I^+ F_J^+ + F_I^\times F_J^\times)$, $\mathcal{R}_{IJ}^V(\hat{\Omega}) \equiv (5/2) \times (F_I^x F_J^x + F_I^y F_J^y)$, and $\mathcal{R}_{IJ}^S(\hat{\Omega}) \equiv [15/(1 + 2\kappa)] \times (F_I^b F_J^b + \kappa F_I^\ell F_J^\ell)$. The subscript M denotes $M = T, V, S$, and $\Delta \vec{X} \equiv \vec{X}_I - \vec{X}_J$.

3 Mode-separation and SNR

The three polarization modes, in principle, can be separated by linearly combining more than three independent correlation signals from detector pairs. In general case with arbitrarily large number N_{pair} of the correlation signal, an SNR by optimally combining the correlation signals is given by [10]

$$\text{SNR}^M = \frac{9H_0^2}{40\pi^2} \left[2T_{\text{obs}} \int_0^\infty df \frac{(\Omega_{\text{gw}}^M(f))^2 \det \mathbf{F}(f)}{f^6 \mathcal{F}_M(f)} \right]^{1/2}, \quad (1)$$

$$\mathbf{F}(f) = \begin{pmatrix} F_{TT} & F_{TV} & F_{TS} \\ F_{TV} & F_{VV} & F_{VS} \\ F_{TS} & F_{VS} & F_{SS} \end{pmatrix}, \quad F_{MM'}(f) = \sum_i \frac{\gamma_i^M(f) \gamma_i^{M'}(f)}{\mathcal{N}_i(f)},$$

where M and M' denote polarization modes, $M, M' = T, V, S$. The quantity \mathcal{F}_M is the determinant of the submatrix, which is constructed by removing the M 's elements from \mathbf{F} . The subscript i designates a detector pair (for I-th and J-th detector pair, $i = IJ$), and $\mathcal{N}_i(f)$ is defined as, say, $\mathcal{N}_{12}(f) \equiv P_1(f)P_2(f)$. The analytical fit of the noise power spectrum of a single interferometer is given by

$$P(f) = \left[6.4 \times 10^{-51} \left(\frac{f}{1\text{Hz}} \right)^{-4} + 1.7 \times 10^{-48} + 5.8 \times 10^{-50} \left(\frac{f}{1\text{Hz}} \right)^2 \right] \text{ Hz}^{-1}.$$

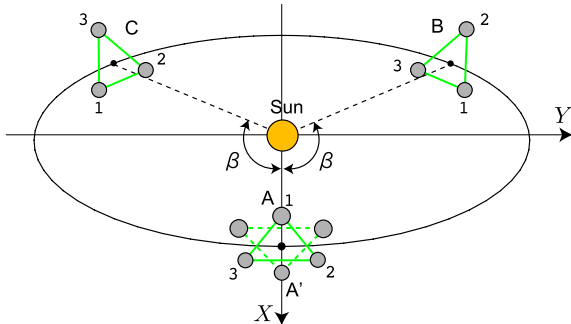


Figure 1: Four clusters, A, A', B, and C, sharing the orbit, whose radius is 1 AU.

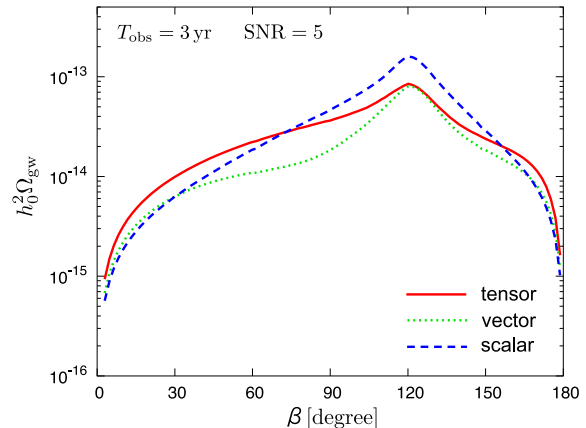


Figure 2: Detectable $h_0^2 \Omega_{\text{gw}}$ ($\xi h_0^2 \Omega_{\text{gw}}$ for the scalar mode) after the mode separation with four clusters of DECIGO.

for DECIGO and

$$P(f) = \begin{cases} 10^{-44} \left(\frac{f}{10 \text{ Hz}} \right)^{-4} + 10^{-47.25} \left(\frac{f}{100 \text{ Hz}} \right)^{-1.7} \text{ Hz}^{-1} & \text{for } 10 \text{ Hz} \leq f \leq 240 \text{ Hz} , \\ 10^{-46} \left(\frac{f}{1000 \text{ Hz}} \right)^3 \text{ Hz}^{-1} & \text{for } 240 \text{ Hz} \leq f \leq 3000 \text{ Hz} , \\ \infty & \text{otherwise .} \end{cases}$$

for advanced LIGO. The mode separability significantly affects the SNR via $\det \mathbf{F}$ in the integrand in Eq. (1). To successfully separate the modes, the condition, $\det \mathbf{F} \neq 0$, is necessary and leads to two conditions that have to be satisfied for the detector configuration: (i) the detectors have to be located at a distance more than one wavelength of the GW, (ii) detector pairs do not geometrically degenerated. If one of the two conditions fails, $\det \mathbf{F} \approx 0$ suppresses the SNR.

In the calculations below, we will assume that $\Omega_{\text{gw}}^M(f)$ has a flat spectrum, *i.e.* frequency-independent, and the observation time is $T_{\text{obs}} = 3 \text{ yr}$. We set the detection threshold to $\text{SNR} = 5$, then it leads to the detectable $h_0^2 \Omega_{\text{gw}}$ ($\xi h_0^2 \Omega_{\text{gw}}$ for the scalar mode).

3.1 Ground-based interferometers

We perform the polarization mode separation with three detectors (minimum set needed to separate modes) among the advanced interferometers on the Earth (at $\sim 100 \text{ Hz}$) such as AIGO, advanced LIGO at Hanford and Livingston, advanced VIRGO, and LCGT. Here we assume that all interferometers have the same noise spectrum as that of advanced LIGO, *i.e.* $P_I(f) = P(f)$. The SNR calculation is straightforward because these interferometers are located on the Earth at the distance more than one wavelength of a GW at $\sim 100 \text{ Hz}$. Therefore, there is no problem concerning the mode degeneracy and the geometrical degeneracy of the detectors. According to [9], the set of three advanced detectors is sensitive to the GWB of $h_0^2 \Omega_{\text{gw}} \sim 10^{-9} - 10^{-8}$ for each polarization. This sensitivity is almost the same as that without the mode separation.

3.2 Space-based interferometers

DECIGO in the current conceptual design [11] is composed of four clusters, orbiting at 1 AU from the Sun, as shown in Fig. 1. Each cluster has three spacecrafts, which form three Fabry-Perot cavity with the armlength 10^3 km . By measuring the relative distance between a pair of the spacecrafts, three interferometer's signals are obtained in a cluster. The correlation signals that we use for the SNR

calculation are those constructed with interferometers of interclusters, because in a cluster, one cannot obtain the correlation signal sensitive enough to a GWB at low frequencies [10].

The detector configuration is shown in Fig. 1. For mathematical details of this configuration, see [10]. Since the detector separation can be approximated as the distance between the guiding centers of clusters, the distances between the clusters $D \equiv |\Delta\vec{X}|$ are unchanged during their orbital motion and are given by $D_{AB}(\beta) = 2R_0|\sin(\beta/2)|$ for the AB link, $D_{AC}(\beta) = D_{AB}(\beta)$ for AC link and $D_{BC}(\beta) = 2R_0|\sin\beta|$ for the BC link. One should be noted that the only parameter in this configuration is β .

In this detector configuration, the detector separation D is typically of the order of 1 AU. This means that the ORF starts to oscillate and rapidly decay above the characteristic frequency, $f_c \equiv c/(2D) \sim 10^{-3}$ Hz. Thus, the large detector separation considerably degrades the sensitivity to the GWB in 0.1 – 1 Hz band, however, since the ORF of each polarization mode oscillates differently in the band, the mode separability is pretty good.

The SNR as a function of β is calculated with, in total, 54 correlation signals (AA', AB, AC, A'B, A'C, BC $\times 9$ links = 54). The result is shown in Fig. 2. At $\beta \sim 120^\circ$, the sensitivity degrades due to the symmetry of the detector configuration, in other words, some correlation signals are degenerated. As β approach 0° and 180° , the detector sensitivity peaks, since the clusters A and B (or C), and B and C are closely located, respectively. However, such a configuration considerably loses the angular resolution to point GW sources. Thus, an optimal angle would be $\beta = 60^\circ$, which leads to $h_0^2\Omega_{\text{gw}}^T = 2.2 \times 10^{-14}$, $h_0^2\Omega_{\text{gw}}^V = 1.1 \times 10^{-14}$, and $\xi h_0^2\Omega_{\text{gw}}^S = 1.9 \times 10^{-14}$. These sensitivities should be compared with those when the polarization modes are not separated. For two clusters that are colocated and coaligned, e.g. clusters A and A', the sensitivity is $h_0^2\Omega_{\text{gw}} = 7.1 \times 10^{-17}$. The mode separation degrades the sensitivity by a few hundred times. However, the important point here is that the non-Einsteinian-polarization search does not impair the cross-correlation sensitivity to a GWB with the colocated and coaligned clusters at all, though the mode is not separated.

4 Conclusion

The GW polarizations can be utilized as a novel and accurate test of gravity. We showed that the ground-based advanced interferometers and the proposed space-based detectors such as DECIGO and BBO can successfully separate and probe the GWB with the non-Einsteinian polarization modes. The GWB search with the GW detectors is complementary to the searches at much different frequencies: CMB and pulsar timing. If the non-Einstein polarizations would be detected, it implies that GR should be extended.

References

- [1] C. M. Will, *Theory and experiment in gravitational physics*, Cambridge University Press (1993).
- [2] C. M. Will, *Living Rev. Relativity* **9**, 3 (2006).
- [3] D. M. Eardley, D. L. Lee, A. P. Lightman, R. V. Wagoner, and C. M. Will, *Phys. Rev. Lett.* **30**, 884 (1973).
- [4] The LIGO Scientific Collaboration and The Virgo Collaboration, *Nature* **460**, 990 (2009).
- [5] N. Christensen, *Phys. Rev. D* **46**, 5250 (1992);
- [6] E. E. Flanagan, *Phys. Rev. D* **48**, 2389 (1993);
- [7] B. Allen and J. D. Romano, *Phys. Rev. D* **59**, 102001 (1999);
- [8] M. Maggiore, *Phys. Rep.* **331**, 283 (2000).
- [9] A. Nishizawa, A. Taruya, K. Hayama, K. Kawamura, and M. Sakagami, *Phys. Rev. D* **79**, 082002 (2009).
- [10] A. Nishizawa, A. Taruya, and S. Kawamura, arXiv:0911.0525 (2009).
- [11] S. Sato *et al.*, *Journal of Physics: Conference Series* **154**, 012040 (2009).